

PAPER • OPEN ACCESS

## Impact of neutrino background prediction for next generation dark matter xenon detector

To cite this article: M Cadeddu and E Picciau 2018 *J. Phys.: Conf. Ser.* **956** 012014

View the [article online](#) for updates and enhancements.

### You may also like

- [New opportunities at the next-generation neutrino experiments I: BSM neutrino physics and dark matter](#)  
C A Argüelles, A J Aurisano, B Batell et al.
- [Neutrino–nucleus cross sections for oscillation experiments](#)  
Teppei Katori and Marco Martini
- [Neutrino physics with JUNO](#)  
Fengpeng An, Guangpeng An, Qi An et al.



The Electrochemical Society  
Advancing solid state & electrochemical science & technology

## 241st ECS Meeting

May 29 – June 2, 2022 Vancouver • BC • Canada

Abstract submission deadline: Dec 3, 2021

Connect. Engage. Champion. Empower. Accelerate.  
**We move science forward**



**Submit your abstract**



# Impact of neutrino background prediction for next generation dark matter xenon detector

M Cadeddu<sup>1,2</sup> and E Picciau<sup>1</sup>

<sup>1</sup> Dipartimento di Fisica, Università degli Studi di Cagliari, S.P. per Sestu, 09042, Italy

<sup>2</sup> INFN-Sezione di Cagliari, Italy

E-mail: emmanuelepicciau1994@gmail.com

**Abstract.** Next generation direct dark matter detectors will have the sensitivity to detect neutrinos from several sources, among which atmospheric and diffuse supernova neutrinos, through the Standard Model reaction of Coherent Elastic Neutrino Scattering on nucleus. This reaction represents an irreducible background that can be expressed as a limit in the Weakly Interacting Massive Particles parameters plane. This limit is known as the “neutrino floor” and it has been obtained by other authors considering standard hypotheses for the neutrino-nucleus form factor and for the coherence of the scattering process. Since the coherent scattering has never been observed experimentally, it is licit to relax some hypotheses in the differential cross section and to evaluate the effect of such modifications on the neutrino floor prediction. In this contribution, we show a more accurate neutrino-nucleus form factor and we discuss the coherence hypothesis of the process in two extreme cases, namely the total coherence and the total decoherence regime. We derive the neutrino background event rate under these new assumptions, considering xenon as a target. The differences between the number of neutrino events and the implication for the next generation dark matter detectors, such as XENON1T/XENONnT, LZ and DARWIN, are discussed.

## 1. Introduction

The presence of Dark Matter (DM) plays a fundamental role at the cosmological and astrophysical scale. So called Weakly Interacting Massive Particles (WIMPs) are considered as the most promising DM candidates. Direct Detection (DD) experiments aim to identify WIMPs by measuring, with different technologies and target materials, the energy deposited by WIMPs after a nuclear recoil. One of the most used technique exploits the effect of scintillation and ionization of liquid nobles (such as xenon and argon) in Time Projection Chambers (TPCs) after a WIMP coherent interaction with nuclei. In this way, one can measure (constrain) two of the unknown WIMP parameters, namely the WIMP-nucleon cross section and the WIMP mass in the case of a positive (null) result. Nowadays, the best upper limit on the WIMP-nucleon cross section has been set by the LUX experiment [1], a Liquid Xenon (LXe) TPC and it is of the order of  $10^{-46}$  cm<sup>2</sup> for a WIMP mass of about 30 GeV/c<sup>2</sup>. In principle, increasing the exposure (the product of the active mass and the live time of the experiment) it is possible to explore lower and lower cross sections. However, it has been pointed out that neutrinos from several sources could scatter off coherently with the whole nucleus producing the same signal of a WIMP [2]. The Coherent Elastic Neutrino Scattering (CENS) process is relatively well described in the Standard Model (SM) framework but it has never been observed experimentally because



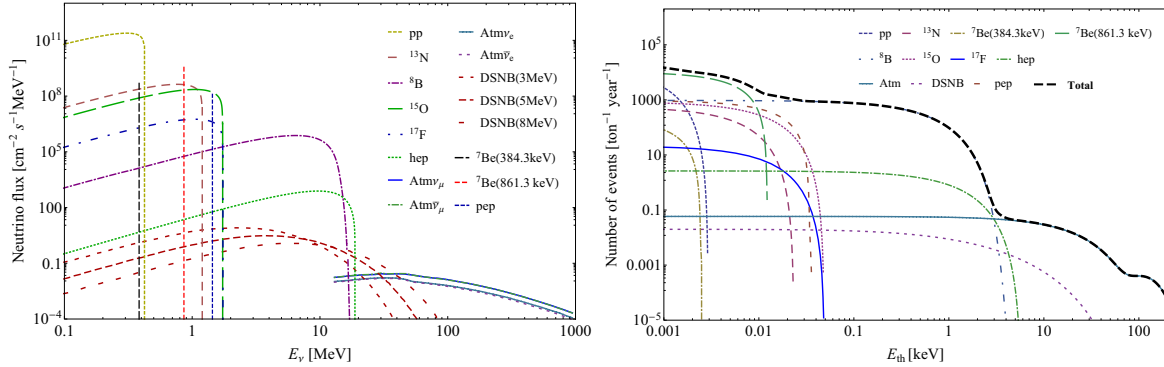


**Figure 1.** (Left panel) Neutrino fluxes on Earth relevant for direct dark matter detection. From low to high energies: solar, diffuse supernova and atmospheric neutrinos. (Right panel) Total number of neutrino background events per unit of ton-year as a function of energy threshold for a xenon target considering  $E_{up} = 400$  keV (dashed black line); partial contributions relative to specific neutrino fluxes are also shown.

the kinematics requires a very low energy threshold to detect it. However, next generation DM experiments will have the potentiality to detect such a process limiting the sensitivity to WIMP discovery. This limit has been quantified by Billard et al [3] which have introduced the concept of *neutrino isoevent contour line*. This line is obtained by drawing on the WIMP-nucleon cross section vs WIMP mass parameters plane the best 90% C.L. exclusion limit achievable at each WIMP mass by a DM experiment for a one neutrino event exposure. This limit depends on the WIMP and neutrino rates which in turn depend on the dynamics of the interactions. In this work, we show the implication of some reasonable modifications to the standard differential cross section for a CENS process that have impact on the number of coherent neutrino background events seen by future DM detectors. In Section 2 we describe the neutrino flux at Earth and the standard formulae for the CENS cross section. In Section 3 we propose the modification of the Helm Form Factor (FF) for the CENS process while in Section 4 we explore the possibility of a partial coherency of the scattering process. Finally, in Section 5 we evaluate the impact on the event rate for both the proposed modifications and in Section 6 we draw our conclusions.

## 2. Neutrino flux and cross section

In this section we evaluate the neutrino background event rate starting from the description of the single neutrino flux components. The main neutrino fluxes at Earth can be divided into three categories: solar, atmospheric and diffuse supernovae neutrinos. Solar neutrinos are produced by the nuclear synthesis reactions inside the Sun such as the proton proton ( $pp$ ) or Carbon-Nitrogen-Oxygen (CNO) chains. They are characterized by energies lower than  $\sim 2$  MeV. The total flux produced in the  $pp$  chain is  $5.94 \times 10^{10} \text{ cm}^{-2} \text{ s}^{-1}$ . Another important contribution is represented by the Diffuse Supernova Neutrino Background (DSNB) generated by all the past supernova explosions in the Universe. The neutrino spectrum of a core-collapse supernova is assumed to be a Fermi-Dirac spectrum with temperatures in the range 3-8 MeV. DSNB flux covers energies up to hundreds of MeV. The last component is constituted by atmospheric neutrinos produced through cosmic ray collisions in the Earth atmosphere. The energy range of interest is approximately 10-1000 MeV. In Fig. 1 (left panel) all the neutrino flux components just mentioned are shown in detail.

As predicted in the SM neutrinos can scatter off coherently with a nucleus through a neutral current process. The coherence of the process is determined by the length scale of the interaction

which in turn is related to the inverse of the momentum exchanged between neutrino and nucleus. The differential cross section depends on the neutrino energy  $E_\nu$  and nuclear recoil energy  $E_r$

$$\frac{d\sigma(E_\nu, E_r)}{dE_r} = \frac{G_f^2}{4\pi} Q_w^2 m_N \left(1 - \frac{m_N E_r}{2E_\nu^2}\right) |F(q^2)|^2, \quad (1)$$

where  $G_f$  is the Fermi coupling constant,  $Q_w = N - (1 - 4\sin^2 \theta_w)Z$  is the weak hypercharge with  $N$  the number of neutrons,  $Z$  the atomic number and  $\theta_w$  is the weak mixing angle. The nucleus mass is denoted by  $m_N$  while  $|F(q^2)|^2$  is the nuclear form factor as a function of the momentum transfer  $q$ . From kinematics it can be shown that the maximum recoil energy and the minimum neutrino energy (in the limit  $m_N \gg E_\nu$ ) are

$$E_r^{max} = \frac{2m_N E_\nu^2}{(m_N + E_\nu)^2} \quad \text{and} \quad E_\nu^{min} = \sqrt{\frac{m_N E_r}{2}}, \quad (2)$$

respectively. The neutrino differential rate and the integrated number of neutrino events are given respectively by

$$\frac{dR}{dE_r} = \eta \times \int_{E_\nu^{min}} \frac{dN}{dE_\nu} \times \frac{d\sigma(E_\nu, E_r)}{dE_r} dE_\nu \quad \text{and} \quad N_\nu(E_{th}) = \int_{E_{th}}^{E_{up}} \frac{dR}{dE_r} dE_r, \quad (3)$$

where  $\eta$  is the number of nucleus targets per unit of detector active mass and  $dN/dE_\nu$  represents the total neutrino flux. The value of  $E_{up}$  represents the upper limit of the nucleus recoil energy. The number of neutrino events per unit of exposure as a function of the energy threshold  $E_{th}$  is shown in Fig. 1 (right panel).

### 3. Form factor modification

In Section 2 we have discussed the differential cross section for the  $\nu$ -nucleus process. The form factor  $|F(q^2)|^2$  introduced in Eq. 1 plays an important role. It takes into account the portion of the nucleus that contributes to the interaction. For this reason it is also connected with the coherency of the process. The result shown in Fig. 1 (right panel) is obtained considering the Helm parametrization of the form factor [4], following the prescription in [3]. This parametrization is certainly suitable for an interaction with equal couplings between the probe and all nucleons as assumed in the standard WIMP-nucleus interaction. However, the neutrino coupling is weighted by the  $Q_w^2$  factor. Thus the contribution of  $\nu$ -proton scattering is lower than the  $\nu$ -neutron one because of the presence of the factor  $(1 - 4\sin^2 \theta_w) \simeq 0.076$ . For this reason it would be better to use a form factor in which this feature is taken into account. Following [5] we propose a new parametrization in the form

$$F(q^2) = \frac{1}{Q_w} [N F_N(q^2) - Z(1 - 4\sin^2 \theta_w) F_Z(q^2)]. \quad (4)$$

The nucleus form factor has been considered as a weighted combination between two different structure functions for the neutron and proton distributions alone,  $F_N(q^2)$  and  $F_Z(q^2)$ . For these single structure functions we use the Helm parametrization described by the following expression

$$|F(q^2)_H|^2 = \left( \frac{3j_1(qR)}{qR} \right)^2 \exp[-q^2 s^2], \quad (5)$$

where  $j_1$  is a spherical Bessel function of the first kind,  $R$  is the effective nuclear radius of the distribution and  $s \simeq 0.9$  fm is the nuclear skin thickness. In this case we need to know the proton and the neutron radius,  $R_Z$  and  $R_N$  respectively. For  $R_Z$  we can use the data of the

nuclear ground state charge radii [6] obtained by combining analyses of optical and absolute radii measured by muonic spectra and electronic scattering experiments. These techniques probe the root-mean-square (rms) nuclear radii of the proton distribution. For the case of xenon ( $N = 77$  and  $Z = 54$ ) we find that  $R_Z \simeq 4.781$  fm.

Since the neutron radius is difficult to probe, with this technique we can estimate it using the following argument. Protons and neutrons are bound together inside a nucleus through strong interaction and so we expect  $R_Z \propto (Z)^{1/3}$  and  $R_N \propto (N)^{1/3}$ . However, protons experience also the repulsive electromagnetic force, thus we expect the neutron radius to be smaller. We parametrize this difference adding a factor  $\alpha$ . Putting all together we can write that

$$R_N = R_Z \cdot \alpha \cdot (N/Z)^{1/3}. \quad (6)$$

For  $\alpha$  we assume a value of 0.9, which means that considering the same number of protons and neutrons the effect of the atomic repulsion would account for a decrease of the radius of the neutrons distribution of 90%. This value is in good agreement with the work of the PREX collaboration [7] in which for the first time the difference between  $R_N$  and  $R_Z$  of  $^{208}\text{Pb}$  has been measured through an electroweak observation. In Fig. 2 (left panel) the comparison between the Helm form factor in Eq. 5 for xenon (red dashed line) and our modification in Eq. 4 for  $\alpha = 0.9$  (solid blue line) is shown. The difference between the two parametrizations is clearly visible.

#### 4. Coherency of the CENS process

In this section we discuss and evaluate the possibility for a transition towards decoherency in a CENS process. The problem has also been studied recently by the TEXONO collaboration [8]. Assuming that the degree of coherency could be quantified by a measurable parameter  $\beta \in [0, 1]$  they obtained that the ratio between the neutrino cross section with a nucleus with  $Z$  protons and  $N$  neutrons ( $\sigma_{\nu-N}$ ) and the cross section of a single neutron ( $\sigma_{\nu-n}$ ) can be written as

$$\frac{\sigma_{\nu-N}}{\sigma_{\nu-n}} = \epsilon^2 Z + N + Z(Z-1)\epsilon^2\beta + N(N-1)\beta - 2ZN\epsilon\beta, \quad (7)$$

where  $\epsilon \equiv 1 - 4\sin^2\theta_w$ . For  $\beta = 1$  the expression in Eq. 7 becomes  $\propto [\epsilon Z - N]^2$ , which represents the full coherency regime, while  $\beta = 0$  implies the opposite condition of total decoherency for which  $\propto [\epsilon^2 Z + N]$ . Notice that in the first case the ratio in Eq. 7 is precisely equal to the weak hypercharge to the square,  $Q_w^2$ .

With these definitions in mind it is possible to evaluate the total cross section,  $\sigma(E_\nu)$ , as a function of the neutrino energy integrating Eq. 1 between zero and  $E_r^{max}$ . In Fig. 2 (right panel) we show the total cross section evaluated combining our modifications to the form factor and to the coherency hypothesis. With the dashed red line it is shown the total cross section (Helm plus full coherency) as used in the Billard et al. paper [3], while with the solid blue line it is shown the prediction obtained when using the form factor presented in Eq. 4 with  $\alpha = 0.9$ . The difference is not so dramatic, however for a neutrino energy in the range 10-100 MeV the inclusion of the proper form factor increases the cross section prediction by a factor 1.007-1.3 respectively. On the contrary, the coherency correction gives a more pronounced effect, lowering the cross section by a flat factor of about 68.7, going from  $\beta = 1$  (full coherency) to  $\beta = 0$  (no coherency).

#### 5. CENS event rate

We now evaluate the impact of our modifications to the differential neutrino event rate in Eq. 3. In Fig. 3 (left panel) it is shown the comparison between the differential number of neutrino background events as a function of the recoil energy per ton-year of a DM xenon experiment for different choices of  $\beta$  and  $\alpha$ . Since the coherency correction does not depends on the energy (see

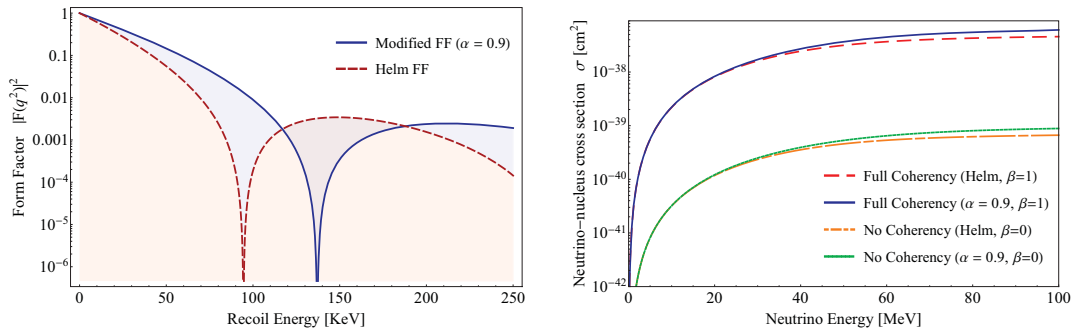


**Figure 2.** (Left panel) Comparison between the standard parametrization of the Helm form factor,  $|F(q^2)_H|^2$ , for a xenon nucleus with dashed red line, and our parametrization of Eq. 4 for  $\alpha = 0.9$  with the solid blue line as a function of the nucleus recoil energy in keV. (Right panel) Integrated cross section for our proposed changes.

Eq. 7), this results in a flat decrease of the differential number of events by a factor  $\sim 68.7$ , which lowers remarkably the number of background with the respect to the standard formula ( $\beta = 1$ ). For  $1 > \beta > 0$  all the possible correction factors between 1 and 68.7 are in principle possible. In the case of the form factor modification the correction is energy dependent and it is less pronounced than the coherency correction. In order to quantify the impact of the implemented correction is better to look at the integrated number of neutrino background events in a given experimental energy window. Driven by a pragmatic motivation, we consider the ratio between the integrated number of neutrino events considering the Helm form factor and the our form factor implementation

$$R(E_{th}) \equiv \int_{E_{th}}^{E_{up}} \frac{(dR^{Helm})}{dE_r} dE_r \bigg/ \int_{E_{th}}^{E_{up}} \frac{(dR^{FF})}{dE_r} dE_r, \quad (8)$$

and we choose some typical values of  $E_{th}$  and  $E_{up}$  for currently ongoing and future xenon experiments such as XENON1T/XENONnT [9], LZ [10] and DARWIN [11]. In Fig. 3 (right panel) it is shown the ratio in Eq. 8 having fixed  $E_{up}$  to 40, 50 and 60 keV, as a function of the threshold energy  $E_{th}$  varying from 2 to 8 keV. The different points represent the particular choice of XENON1T (green triangle), XENONnT (blue cross), LZ (black star) and DARWIN (red disk) for which  $R$  has the value of 0.77, 0.78, 0.87 and 0.78 respectively. This means that the relative correction to the number of neutrino background events is between 15-30% for the most used value of  $E_{up}$  and  $E_{th}$ . For example, in the case of DARWIN which aims to reach an exposure of 200 tonne year, the integrated number of neutrino background events will be 12.8 instead of 10. This would result in a significant change of the sensitivity or of the discovery limit of WIMPs. Indeed, since the neutrino and WIMP spectra match relatively well, in the case of a significant neutrino contribution it can be shown [3] that the WIMP discovery limit goes like  $\sigma_{CL} \propto \sqrt{(1 + \xi^2 N_\nu)/N_\nu}$ , where  $\xi$  is the systematic error in percentage on the neutrino contribution. Considering that the neutrino flux uncertainty of the two neutrino components of interest, namely atmospheric and DSNB, is quite big (20% and 50% respectively), it is of vital importance to reduce as much as possible the uncertainties on the cross section inputs, the uncertainties related to the neutron distribution radius and to find the right coherence dependence with a dedicated experimental campaign.

## 6. Conclusions

In this work we discuss how modifications to the neutrino-nucleus form factor and the coherency hypothesis of CENS process could lead to sizeable change of the neutrino irreducible background.



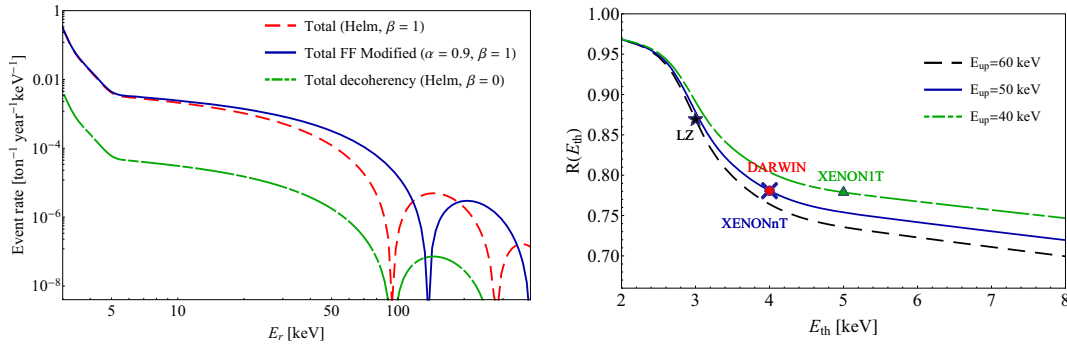


**Figure 3.** (Left panel) Neutrino event rate as a function of the recoil energy  $E_r$ . The dashed red line represents the standard prediction, the solid blue line is the prediction with the inclusion of the proper form factor ( $\beta = 1$ ), while the dash-dotted green line represents the differential rate for total decoherency regime ( $\beta = 0$ ) and with a Helm form factor. (Right panel) Ratio between the integrated number of neutrino events considering the standard cross section and the form factor correction as a function of the threshold energy (see Eq. 8). We fix  $E_{up}$  to 40, 50 and 60 keV, and we show the ratio as a function of the threshold energy  $E_{th}$ . The different points represent the particular choice of  $E_{th}$  made by XENON1T (green triangle), XENONnT (blue cross), LZ (black star) and DARWIN (red disk).

We show, first of all, that the adoption of the Helm form factor, as done in [3], is not suitable for the case of CENS. Neutrinos couple preferentially with neutrons, therefore probing more the neutron distribution than the proton one. We propose to use a form factor obtained by a weighted combination between the two structure functions of the neutron and of the proton,  $F_N(q^2)$  and  $F_Z(q^2)$ . Since  $F_N(q^2)$  has not been precisely determined yet we propose a simple parametrization to estimate it. We thus evaluate the differential neutrino spectrum and the total number of neutrino events. We have shown that the usage of our form factor increases the number of background neutrino events by a factor 15-30% in the case of future xenon DM experiments like XENON1T, XENONnT, LZ and DARWIN. We consider also the possibility for the CENS process not to be completely coherent including a coherency correction factor  $\beta$ . This correction gives a more substantial effect on the predicted number of neutrino events lowering it down to a factor  $\sim 68.7$  in the case of total decoherence ( $\beta = 1$ ). All these corrections to the CENS cross section prediction substantially change the neutrino isoevent contour line [12]. Since the WIMP discovery limit depends crucially on the uncertainty in the neutrino background prediction, it is of utmost importance to perform a dedicated measure of the CENS.

## References

- [1] Akerib D S *et al* 2016 *Phys. Rev. Lett.* **116** 161301
- [2] Freedman D Z 1974 *Phys. Rev. D* **9** 1389
- [3] Billard J *et al* 2014 *Phys. Rev. D* **89** 023524
- [4] Helm R 1956 *Phys. Rev.* **104** 1466
- [5] Amanik P S and McLaughlin G C 2009 *J. Phys. G* **36** 015105
- [6] Angeli I and Marinova K P 2013 *Atomic Data and Nuclear Data Tables* **99** Pages 69-95
- [7] Hagen G *et al* 2016 *Nature Physics* **12**, 186190
- [8] Kerman S 2016 *Phys. Rev. D* **93** 113006
- [9] Aprile E *et al* XENON Collaboration 2016 JCAP04 027
- [10] Akerib D S *et al* LUX-ZEPLIN Collaboration 2015 arXiv:1509.02910 [physics.ins-det]
- [11] Aalbers J *et al* 2016 JCAP 1611 no.11, 017
- [12] Cadeddu M and Picciau E 2017 (in preparation)